Sensors and Materials, Vol. 37, No. 10 (2025) 4323–4334
MYU Tokyo

S & M 4184

Synthesis of Chromium (III) Oxide by Pyrolysis of CrO_3–phenylalanine Precursor: Structural, Spectroscopic, and Morphological Properties of Green Cr_2O_3 Oxide Nanostructure

Sattam Al-Otaibi*

Department of Electrical Engineering, College of Engineering, Taif University,
P.O. Box 11099, Taif 21944, Saudi Arabia

(Received May 19, 2025; accepted July 29, 2025)

Keywords: nanosized Cr_2O_3 oxide, phenylalanine, precursor, XRD, TEM

With the CrO_3−phenylalanine complex as a precursor, pyrolysis was successfully used to create a rhombohedral green chromium oxide (Cr_2O_3-NP) nanostructure. As a clean process, CrO_3 oxide and phenylalanine amino acid were subjected to solid–solid grinding for 1 h to create the CrO_3−phenylalanine precursor. After characterization by infrared spectroscopy and microanalysis, the solid precursor compound was annealed for 3 h in static air at 600 °C in a muffle furnace. FT-IR spectroscopy, Raman laser spectroscopy, SEM, energy-dispersive X-ray spectroscopy (EDX), TEM, and X-ray powder diffraction (XRD) were all used to thoroughly characterize the resulting Cr_2O_3-NP. The existence of crystalline Cr_2O_3 is evident from the Fourier-transform infrared (FTIR) peak characteristic vibrations of Cr−O and two characteristic peaks at 646 and 568 cm^{-1} that are ascribed to Cr−O stretching modes, according to the results of spectral analysis. Since no distinctive impurity peaks were found, the FT-IR and XRD data demonstrated that the Cr_2O_3-NPs are pure and have an excellent crystalline structure. A UV–Vis spectrophotometer was used to quantify the energy band gap (4.80 eV) of the chromium (III) oxide nanostructures. A significant amount of nanostructure with an average crystal size of 5–7 nm was discovered using TEM and picture data, proving that this synthesis approach is an effective way to create Cr_2O_3 nanoparticles.

1. Introduction

Nanochemistry, one of the contemporary sciences, has found extensive use in the fields of energy and pollution, as well as in numerous industrial, medical, and agricultural applications.[1,2] One of the main economic and environmental remedies for the rising rates of pollution caused by fossil fuels and other conventional energy sources is still renewable energy or green chemistry.[3] Sunlight, which is readily available and natural, is frequently employed to save energy in green chemical reactions.[4] Of all renewable energy sources, solar energy remains the most abundant

*Corresponding author: e-mail: srotaibi@tu.edu.sa; dr.sattam.alotaibi@gmail.com
https://doi.org/10.18494/SAM5737

ISSN 0914-4935
https://myukk.org/

and pure. Solar cells, also referred to as photovoltaics, are devices that employ this energy to transform solar radiation into electrical power. Owing to the unique composition of solar cells, which generate current by allowing free electrons to travel in a single direction, photovoltaic material energy incidents create electron–hole pairs to overcome the energy band gap of the photovoltaic equipment and allow the current to flow, typically in the p-n (semiconductor) junction.[5]

The production of nanostructures has advanced significantly in recent decades. Transitional metal oxides are nanomaterials that are crucial to chemistry, physics, materials science, and technology applications.[6] Metal oxides are frequently utilized as catalysts and in the production of sensors, electronic circuits, fuel cells, and coatings for surfaces resistant to corrosion.[7] Because of their size and high density of edge surface locations, metal oxide nanostructures can have special chemical characteristics.[8] Chromium nanostructure (III) (Cr_2O_3) is one of the inorganic nanostructures that has drawn the most attention because of its many potential uses, such as pigment[9] and heterogeneous catalysts,[10] coating materials for biological applications,[11,12] digital recording systems,[13] photonic and electronic devices,[14] and thermal protection.[12] The formation of the Cr_2O_3 nanostructure was accomplished by several methods, including hydrothermal synthesis,[15] solid pyrolysis,[16] combustion,[17] sol-gel technology,[18] precipitation,[19] chromium oxidation,[20] laser-induced deposition,[21] mechanochemical reaction and subsequent heat treatment,[22] and sonochemical methods.[23] Cr_2O_3 nanostructures were prepared by a variety of techniques, including sol-gel technology, laser-induced deposition, hydrothermal reduction, chemical-mechanical reaction, condensation–polymerization, gas condensation, solid pyrolysis, homogeneous precipitation with urea, microwave plasma, sonochemical reaction, thermal treatments, nanocasting, hydrazine reduction, and solution-combustion synthesis.[24]

By reducing potassium dichromate solution with leaf extracts from *Tridax procumbens*[25] and *Allium sativum*,[26] Cr_2O_3 NPs were created. By utilizing an extract from *Callistemon viminalis* flowers, pure, uniformly sized Cr_2O_3 NPs with a cubic shape were created by a green chemistry technique.[27] Pumpkin leaf extract was combined with potassium dichromate solution to create Cr_2O_3-NPs. After 6 h of drying at 70 °C, the solution was calcined at 650 °C.[28] An environmentally acceptable method that uses natural reducing and capping agents is the use of bioorganisms.[29] Colorants, coatings, catalysts, green pigments, solar energy collectors, and liquid crystal displays are just a few of the many uses of chromium oxide nanoparticles.[30]

In this work, we synthesized chromium oxide nanoparticles by pyrolysis using a CrO_3–phenylalanine complex as a precursor. The synthesized nanoparticles were characterized by X-ray diffraction, SEM, and UV–Vis techniques.

2. Experimental Methods

2.1 Materials

Every synthesis material was purchased commercially and used just as supplied with no additional purification.

2.2 Measurements

A Perkin Elmer CHN 2400 was used for microanalysis. The Bruker Fourier-transform infrared (FTIR) spectrophotometer (4000–400 cm^{-1}) was used to record infrared spectra. The Bruker FT Raman was used to measure Raman laser spectra with a 50 mW laser. The UV2 Unicam UV/Vis spectrophotometer was used to scan the electronic spectra. Quanta FEG 250 equipment was used to capture images by SEM. A Bruker D8 Advance X-Ray diffractometer with a Cu Kα anode (λ = 0.1542 nm) running at 40 kV and 30 mA was used to record X-ray diffraction (XRD) patterns. These patterns were obtained within an angular range of 5 to 60° and at 25 °C. A JEOL 100s microscope was used to create TEM images.

2.3 Synthesis

In an agate mortar, 1 mmole of chromium trioxide (CrO_3) and 1 mmole of phenylalanine were ground separately for 15 min. For 1 h, the brown fine powder reactant was combined and ground (Scheme 1). For 3 h, the solid product was annealed in an oxygen environment at 600 °C in a muffle furnace. A closed glass bottle was used to store the chromium (III) oxide Cr_2O_3-NPs until the spectroscopic and morphological analyses were started.

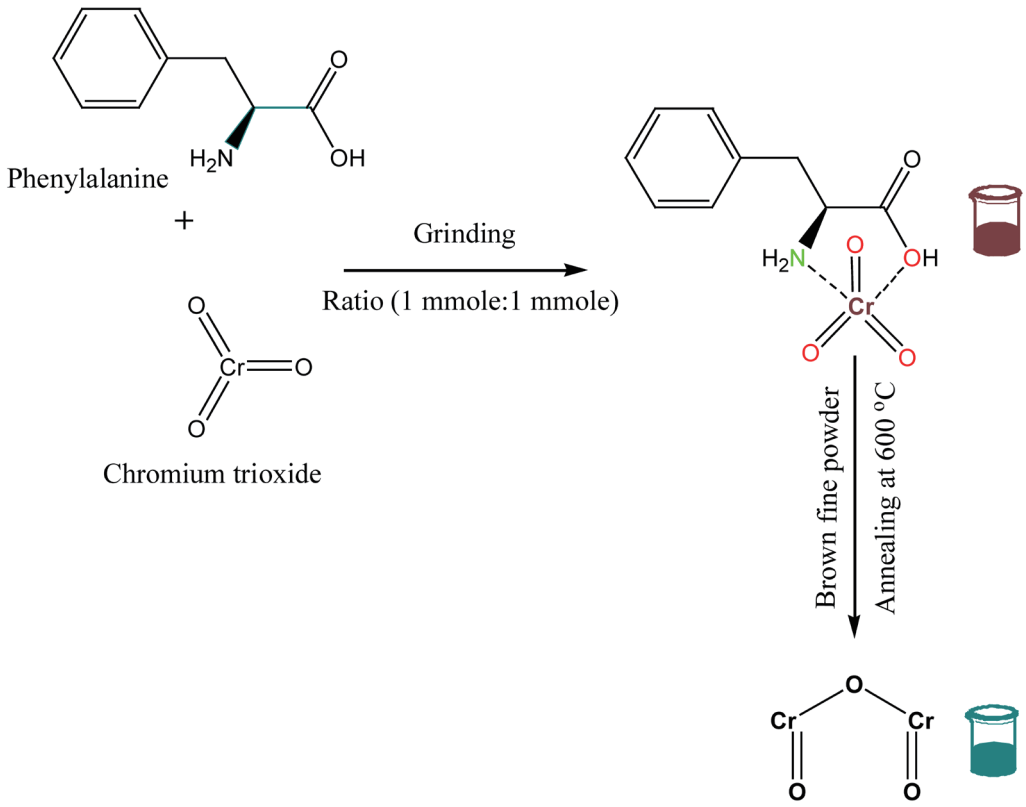

Scheme 1. (Color online) Synthesis pathway of CrO_3–phenylalanine complex precursor and Cr_2O_3–NPs.

3. Results and Discussion

3.1 Preface

The brown formed CrO_3–phenylalanine complex was practically soluble in water and common organic solvents but was found to be soluble in diluted mineral acids at room temperature. Phenylalanine was found to coordinate with CrO_3 as a bidentate ligand through the nitrogen of the amino group and the oxygen of the carboxylic group with a 1:1 molar ratio. The elemental analysis of the CrO_3–phenylalanine [$CrO_3(C_9H_{11}NO_2)$] complex can be summarized as follows: Anal.: found C, 40.62; H, 4.11; N, 5.20; Cr, 19.44, Calcd.: C, 40.76; H, 4.18; N, 5.28; Cr, 19.61. The CrO_3–phenylalanine complex is diamagnetic and is produced by treating chromium trioxide with phenylalanine. According to microanalytical and infrared spectroscopy, the complex is 5-coordinate. The proposed mechanism for the thermal decomposition of the CrO_3–phenylalanine complex is

$$2[CrO_3.C_9H_{11}NO_2] \xrightarrow{600\ ^oC} Cr_2O_3 + 6C_2H_2 + 6CO + H_2O + 2NH_3 + H_2. \quad (1)$$

3.2 FTIR and Raman studies

Figure 1 shows the FTIR spectra of the CrO_3–phenylalanine complex precursor and chromium oxide (Cr_2O_3) sample prepared by pyrolysis. The characteristic absorption peaks at

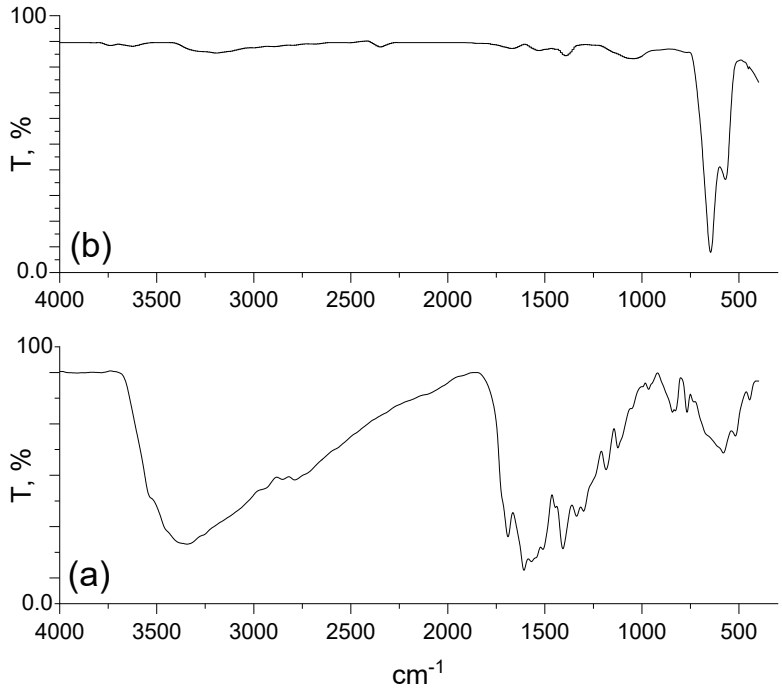

Fig. 1. FTIR spectra of (a) CrO_3–phenylalanine complex precursor and (b) as-prepared Cr_2O_3-NPs.

1688 and 1299 cm^{-1} may be attributed to the C=O and C–O stretching frequencies of the carboxyl group of phenylalanine, respectively. The absorption peaks at 1336, 1406, 1505 and 1567 cm^{-1} are probably due to the ν(COO) stretching frequency of the carboxyl group of phenylalanine. The absorption of the O–H stretching of the carboxyl group appeared as a broad band at 3360 cm^{-1}. The absorption peaks at 2946, 2860, and 2799 cm^{-1} were due to the C–H stretching (phenyl and aliphatic CH_2 groups). The vibrational frequency at 1607 cm^{-1} is assigned to ν(C=C) of the aromatic ring. The symmetric and asymmetric stretching vibrations of the COO group were observed at 1567 cm^{-1} as a weak peak and at 1406 cm^{-1} as a strong peak. The sharp absorption band at 3697 cm^{-1} is assigned to the O–H carboxyl group of phenylalanine. This band was shifted to a lower wavenumber (3360 cm^{-1}) after complexation due to the involvement of the oxygen atom of the carboxyl group in the coordination process. The infrared spectrum of the CrO_3–phenylalanine complex has detected bands within the 443–674 cm^{-1} range, and these are attributed to ν(Cr-O) and ν(Cr-N), according to the coordination between CrO_3 and phenylalanine. It is evident that the broad band at 3202 cm^{-1} agrees with the stretching modes of the OH group of the crystalline water molecules. Upon the annealing of the CrO_3–phenylalanine complex at 600 °C, Cr_2O_3 absorption bands appeared below 1000 cm^{-1} owing to interatomic vibrations. The two sharp peaks present at 646 and 568 cm^{-1} attributed to ν(Cr-O) stretching modes are clear evidence of the presence of crystalline Cr_2O_3.[31] Raman shifts (Fig. 2) at 668, 555, 504, 447, 365, and 303 cm^{-1} can be assigned to the Raman modes of Cr_2O_3.[31] There are two medium bands found at 925 and 975 cm^{-1}, which are assigned to the combination band (two or more states excited simultaneously). Cr_2O_3 has the corundum-type structure of the space group *R*-3*c*, with hexagonal close-packed layers of oxygen atoms and two-thirds of the octahedral holes in between filled by chromium atoms. It belongs to the D^6_{3d} space group, and the irreducible representations for the optical modes in the crystal are $2A_{1g} + 2A_{1u} + 3A_{2g} + 2A_{2u} +$

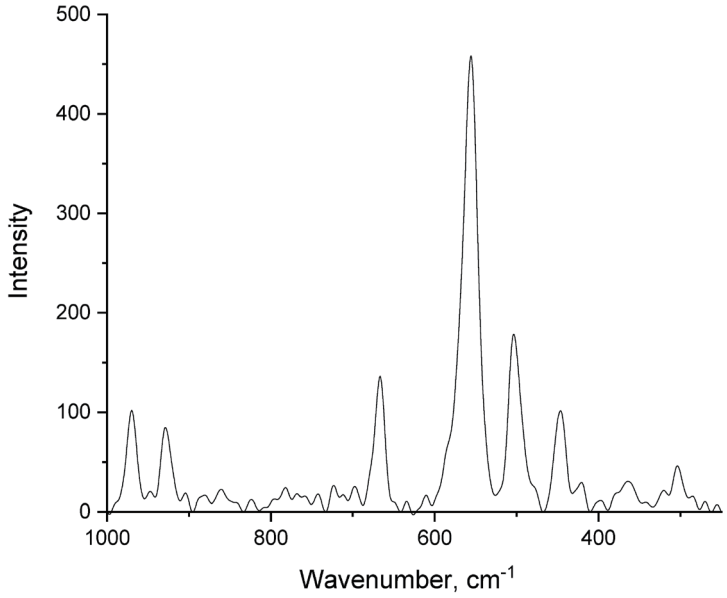

Fig. 2. Raman spectrum of as-prepared Cr_2O_3-NPs.

$5Eg + 4Eu$. Vibrations with symmetry A_{1g} and Eg are Raman-active, which means that there are six Raman active modes. The most intense peak at 555 cm^{-1} corresponded to the ν_1 (A_{1g}) vibration mode of chromia. Another two sharp peaks at 668 and 447 cm^{-1}, as well as two weak peaks at 504 and 365 cm^{-1}, were due to the Eg vibration modes. A sharp peak at 303 cm^{-1} was attributed to the A_{1g} mode.[32]

3.3 UV–Vis spectra and optical studies

The UV–Vis absorption spectrum of Cr_2O_3-NPs has three detected peaks at 295, 395, and 610 nm as shown in Fig. 3. The band gap transition of Cr^{4+} is represented by the absorption at 295 nm, whereas the electronic transition state from $^4A_{2g}$ $^4T_{1g}$ and $^4A_{2g}$ $^4T_{2g}$ of Cr^{3+} is attributed to the additional two peaks at 395 and 610 nm, respectively. These values are consistent with the values reported in Ref. 32 and are situated in six-coordinate geometry and octahedral symmetry.[33]

The electronic absorption spectrum of the synthesized Cr_2O_3 nanostructure is shown in Fig. 3. The spectrum shows the general direction of absorption, that is, a material absorbs less when the frequency of incident light decreases. For the synthesized Cr_2O_3-NPs, Fig. 4 shows the change in $(h\nu\alpha)^2$ with photon energy ($h\nu$). According to Ref. 33, the figure shows a direct band gap of about 4.80 eV.[34]

3.4 XRD analysis

The XRD patterns (2θ = 5–60°) of as-prepared Cr_2O_3-NPs are shown in Fig. 5. The six prominent, intense, and characteristic peaks of the synthesized Cr_2O_3-NPs located at 2θ = 24,

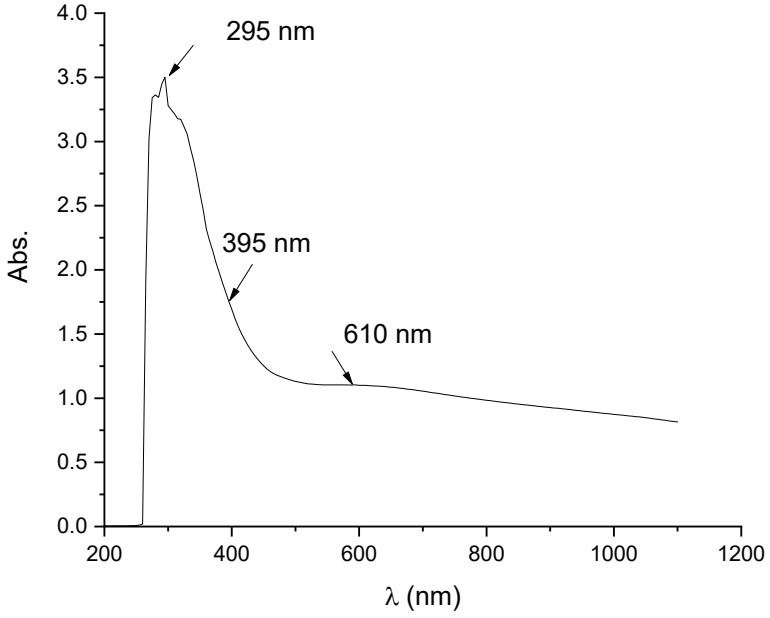

Fig. 3. UV-Vis absorption spectrum of as-prepared Cr_2O_3-NPs.

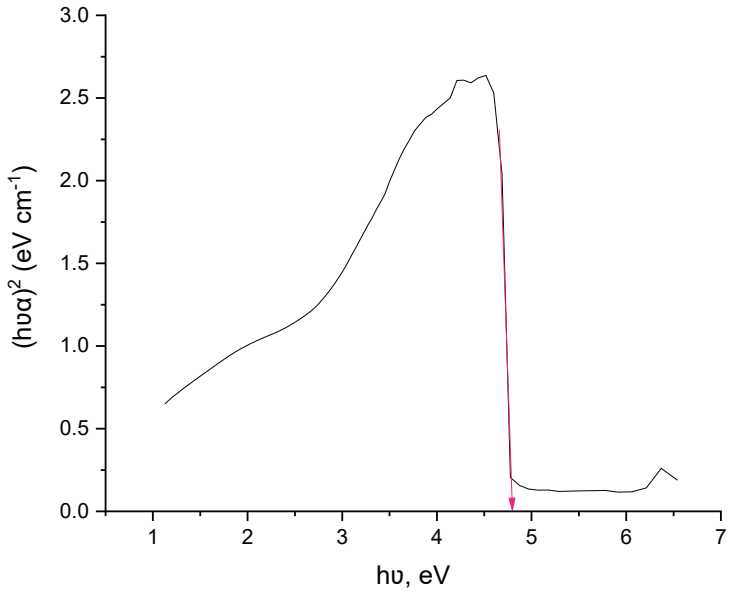

Fig. 4. (Color online) Tauc plot for the direct band gap of as-prepared Cr_2O_3-NPs.

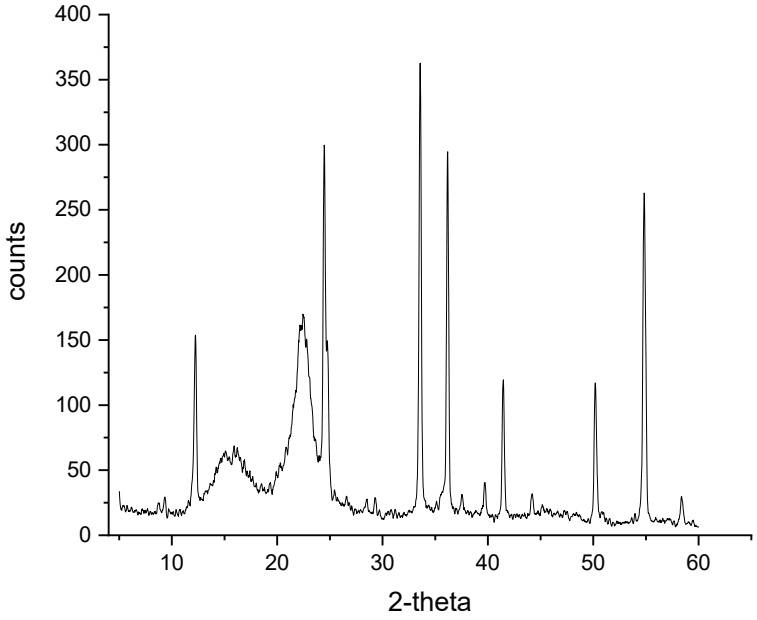

Fig. 5. XRD spectrum of as-prepared Cr_2O_3-NPs.

34, 36, 39, 41, 45, 50, 55, and 58°, which were indexed by their (012), (104), (110), (006), (113), (202), (024), (116) and (122) indices, respectively. All the peaks can be assigned to Cr_2O_3 oxide based on the information provided by card number 00-038-1479. The Scherrer equation $D = K\lambda/(\beta \cos \theta)$, where λ = 1.54056 Å is the X-ray wavelength, K = 0.9 is the Scherrer constant (β), FWHM is the full width at half-maximum, and (θ) is the Bragg diffraction angle.[35,36]

3.5 Morphological analysis

SEM was used to assess the morphological features of the solid-state aggregation of the produced Cr_2O_3-NPs by applying an electron acceleration voltage of 20 kV. The SEM image of the synthesized Cr_2O_3-NPs at 150× magnification is shown in Fig. 6. The rough surface morphology indicates a high surface area, which is typical for nanoparticles.

The presence of Cr_2O_3-NPs was verified by EDX analysis. Their O content was 27.0% and their Cr content was 73%. Chromium oxide nanoparticles are extremely pure, with no traces of contaminants, according to the results of elemental analysis (Fig. 7).

Figure 8 shows the distinct morphology of the Cr_2O_3 nanostructure created using a TEM image. A significant amount of nanostructure (NPs) with an average crystallite size of 5–7 nm can be seen in the image findings, indicating that our synthesis approach is a successful way to manufacture Cr_2O_3-NPs.

A comparison between the present study with conventional or other green synthesis methods can be discussed with the following points:

Superior Size Control

- The present method achieved sub-10 nm particle size, which is extremely good in green synthesis.
- Most studies show Cr_2O_3 nanoparticles within the 15–40 nm size range, even with optimized plant extract methods.
- This suggests better nucleation control or slower growth kinetics in our amino acid-based pyrolysis approach.

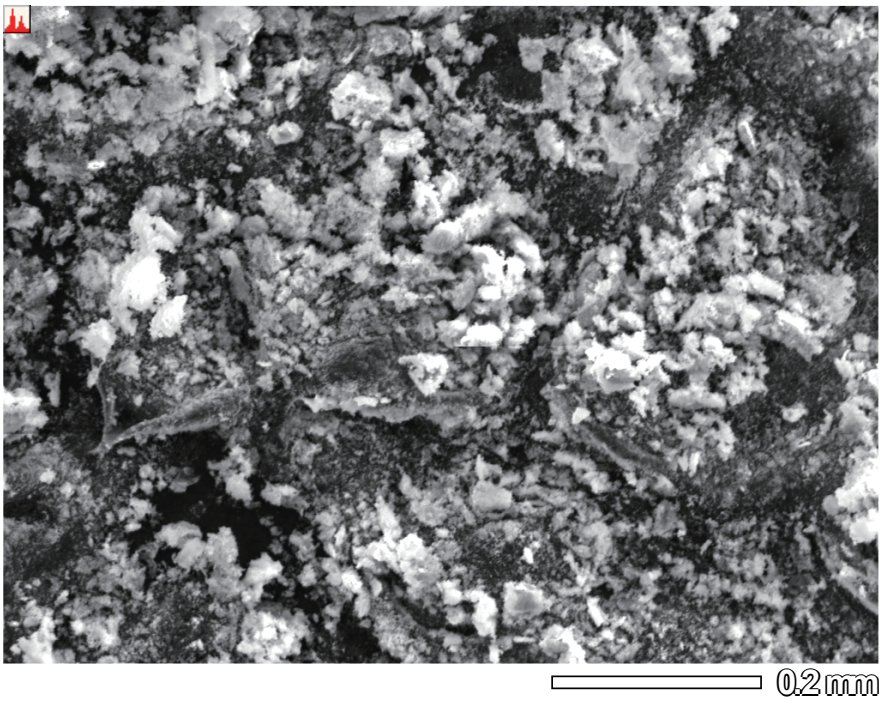

Fig. 6. (Color online) SEM image of as-prepared Cr_2O_3-NPs.

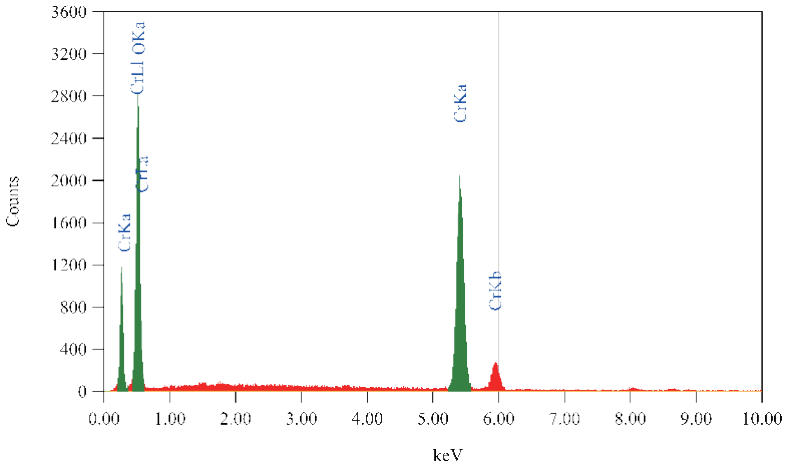

Fig. 7. (Color online) EDX spectrum of as-prepared Cr_2O_3-NPs.

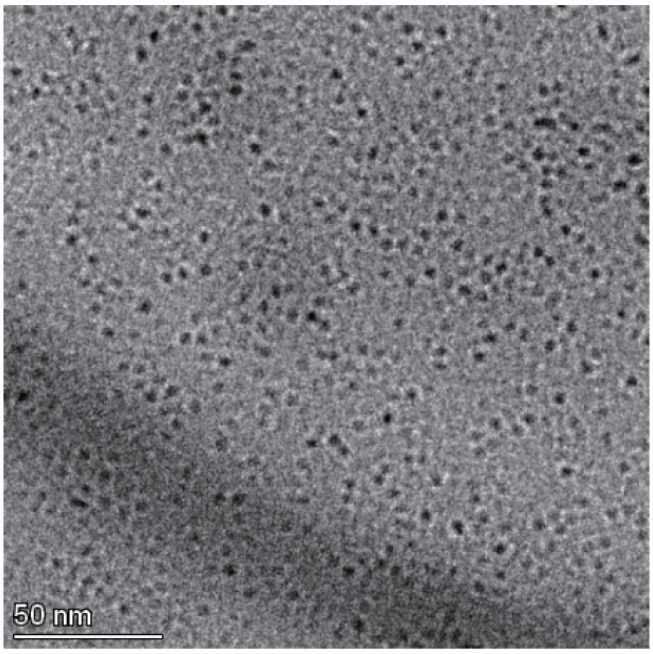

Fig. 8. TEM image of as-prepared Cr_2O_3-NPs.

Green Chemistry Innovation

- Using amino acids as a single-source precursor (carbon + nitrogen) is less common than using plant extracts.
- The present synthesis method avoids complex extracts or multistep procedures, making it a cleaner, reproducible, and more controlled green route.

Higher Surface Area Potential

- Particles in the 5–7 nm size range generally have a much higher surface-area-to-volume ratio than those in the 20–30 nm size range.

- This potentially enhances reactivity, adsorption capacity, and catalytic efficiency, which can outperform many literature-reported Cr_2O_3 materials.

Possible Improved Functional Properties

- Smaller Cr_2O_3 nanoparticles often show better antibacterial, photocatalytic, and electrochemical properties.
- The synthesized Cr_2O_3 nanoparticles may exhibit a higher activity at lower doses or shorter exposure times than larger particles.
- Crystalline nanoparticles <10 nm in size are difficult to obtain without sacrificing structural order, so if this is achieved, it is a major advantage.

Thermal Stability Implications

- Smaller particles often have a lower thermal stability. However, pyrolysis can enhance stability by forming a stronger crystalline phase.
- The present synthesis process may have balanced particle miniaturization and phase stability, a key achievement.

Cost-effectiveness & Scalability

- Amino acids are inexpensive and biodegradable, which may make processes more economically scalable than those relying on plant extracts, which vary in composition.
- The present method can be more easily optimized and industrialized.

Environmental & Biomedical Relevance

- With small particle size and green precursors, synthesized Cr_2O_3 may be well suited for biomedicines (e.g., antimicrobial agents and drug delivery), sensors (high sensitivity due to small size), energy storage (higher surface area improves charge transfer), and catalysis (active sites maximized per gram).

4. Conclusions

In this work, we demonstrated that the pyrolysis approach, employing the CrO_3-phenylalanine complex as a precursor, was successful in producing chromium oxide nanoparticles. The synthesized Cr_2O_3 NPs are between 5 and 7 nm in size, according to the results of TEM analysis. EDX demonstrated that the produced nanoparticles are pure and that the samples contain no traces of contaminants. Applications for chromium oxide nanoparticles include the stropping of knives, glassware, paints, inks, and precursors to magnetic pigments.

Acknowledgments

The author extends his appreciation to Taif University, Saudi Arabia, for supporting this work through project number TU-DSPP-2024-100.

Funding

This research was funded by Taif University, Saudi Arabia (Project no. TU-DSPP-2024-100).

References

1 A. A. Ali, R. M. Al-Hassani, D. H. Hussain, A. M. Rheima, and H. S. Meteab: Drug Inven. Today **14** (2020) 31.
2 A. H. Ismail, H. K. Al-Bairmani, Z. S. Abbas, and A. M. Rheima: Nano Biomed. Eng. **12** (2020) 253. https://doi.org/10.5101/nbe.v12i3.p253-261
3 A. A. Ali, R. M. Al-Hassani, D. H. Hussain, A. M. Rheima, A. N. Abd, and H. S. Meteab: J. Southwest Jiaotong Univ. **54** (2019) 1. https://doi.org/10.35741/issn.0258-2724.54.6.13
4 A. H. Ismail, H. K. Al-Bairmani, Z. S. Abbas, and A. M. Rheima: J. Xian Univ. Archit. Technol. **12** (2020) 2775.
5 S. H. Jabber, D. H. Hussain, A. M. Rheima, and M. Faraj: Al-Mustansiriyah J. Sci. **30** (2019) 94. https://doi.org/10.23851/mjs.v30i1.389
6 K. Gesheva, T. Ivanova, G. Bodurov, I. M. Szilagyi, and N. Justh: J. Phys. Conf. Ser. **682** (2016) 012011. https://doi.org/10.1088/1742-6596/682/1/012011
7 M. Fernandez-Garcia, A. Martinez-Arias, J. C. Hanson, and J. A. Rodriguez: Chem. Rev. **104** (2004) 4063. https://doi.org/10.1021/cr030032f
8 A. A. Oun, Sh. Shankar, and J. W. Rhim: Crit. Rev. Food Sci. Nutr. **60** (2019) 435. https://doi.org/10.1080/10408398.2018.1536966
9 D. Hebbar, K. S. Choudhari, S. A. Shivashankar, C. Santhosh, and S. D. Kulkarni: J. Alloys Compd. **785** (2019) 747. https://doi.org/10.1016/j.jallcom.2019.01.254
10 R. Karimiana and F. Pirib: J. Nanostruct. **13** (2013) 87. https://doi.org/10.7508/jns.2013.01.010
11 T. Chang, X. Cao, N. Li, S. Long, X. Gao, L. R. Dedon, G. Sun, H. Luo, and P. Jin: ACS Appl. Mater. Interfaces **9** (2017) 26029. https://doi.org/10.1021/acsami.7b07137
12 S. P. Singh, S. Chinde, S. S. Kamal, M. F. Rahman, M. Mahboob, and P. Grover: Environ. Sci. Pollut. Res. **23** (2015) 3914. https://doi.org/10.1007/s11356-015-5622-0
13 D. Hassan, A. T. Khlil, A. R. Solangi, A. El-Mallul, Z. K. Shinwari, and M. Maaza: Appl. Organomet. Chem. **33** (2019) e5041. https://doi.org/10.1002/aoc.5041
14 M. D. Bijker, J. J. J. Bastiaens, E. A. Draaisma, L. A. M. de Jong, E. Sourty, S. O. Saied, and J. L. Sullivan: Tribol. Int. **36** (2003) 227. https://doi.org/10.1016/S0301-679X(02)00191-3
15 X. He and D. Antonelli: Angew. Chem. Int. Ed. **114** (2002) 222. https://doi.org/10.1002/1521-3757(20020118)114:2<222::AID-ANGE222>3.0.CO;2-5
16 A. El-Trass, H. Elshamy, I. El-Mehasseb, and M. El-Kemary. Appl. Surf. Sci. **258** (2012) 2997. https://doi.org/10.1016/j.apsusc.2011.11.025
17 K. Mohanapandian and A. Krishnan: Int. J. Adv. Eng. Technol. **7** (2016) 273.
18 H. Wang, W. Han, X. Li, B. Liu, H. Tang, and Y. Li: Molecules. **24** (2019) 361. https://doi.org/10.3390/molecules24020361
19 H. I. Abdullah and L. J. Abbas: Int. J. Appl. Phys. and Bio-Chemistry Res. **7** (2017) 1.
20 S. Tian, X. Ye, Y. Dong, W. Li, B. Zhang, B. Li, and H. Feng: Int. J. Electrochem. Sci. **14** (2019) 8805. https://doi.org/10.20964/2019.09.21
21 F. Piri, N. Shakour, M. Zandi, R. Karimian: J. Nanostruct. **1** (2011) 39. https:///doi.org/10.7508/jns.2011.01.006
22 T. Tsuzuki and P. G. Mc Cormick: Acta Mater. 48 (2000) 2795. https://doi.org/10.1016/S1359-6454(00)00100-2
23 L. M. Alrehaily, J. M. Joseph, and J. C. Wren: J. Phys. Chem. C **119** (2015) 16321. https://doi.org/10.1021/acs.jpcc.5b02540
24 M. M. Abdullah, M. R. Fahd, and S. M. Al-Abbas: AIP Adv. **4** (2014) 027121. https://doi.org/10.1063/1.4867012
25 C. Ramesh, K. M. Kumar, N. Latha, and V. Ragunathan: Curr. Nanosci. **8** (2012) 603. https://doi.org/10.2174/157341312801784366
26 T. Satgurunathan, P. S. Bhavan, and R. D. S. Joy: Biol. Trace Elem. Res. **187** (2019) 543. https://doi.org/10.1007/s12011-018-1407-x.
27 B. T. Sone, E. Manikandan, A. G. Fakim, and M. Maaza: Green Chem. Lett. Rev. **9** (2016) 85. https://doi.org/10.1080/17518253.2016.1151083
28 N. Gupta and S. P. Resmi: Imperial J. Interdiscip. Res. **2** (2016) 2454. https://www.researchgate.net/profile/Resmi_S_P/publication/309040610
29 S.-Y. Cheah, M. Aminuzzaman, Y.-K. Phang, S. C. Y. Lim, and M. X. Koh: Green Process. Synth. **14** (2025) 20240246. https://doi.org/10.1515/gps-2024-0246.
30 V. Balouria, A. Singh, A. K. Debnath, A. Mahajan, R. K. Bedi, D. K. Aswal, and S. K. Gupta: AIP Conf. Proc. **1447** (2012) 341. https://doi.org/10.1063/1.4710019
31 D. A. Brown, D. Cuhningham, and W. K. Glass: Spectrochim. Acta, Part A **24** (1968) 965. https://doi.org/10.1016/0584-8539(68)80115-1

32 J. Yang, H. Cheng, W. Martens, and R. Frost: J. Raman Spectrosc. 42 (2011) 1069. https://doi.org/10.1002/jrs.2794
33 B. B. Kamble, M. Naikwade, K. M. Garadkar, R. B. Mane, K. K. K. Sharma, B. D. Ajalkar, and S. N. Tayade: J. Mater. Sci.: Mater. Electron. **30** (2019) 13984. https://doi.org/10.1007/s10854-019-01748-5
34 M. Julkarnain, J. Hossain, K. S. Sharif, and K. A. Khan: Canad. J. Chem. Eng. Technol. **3** (2012) 81.
35 I. F. Al-sharuee and F. H. Mohammed: IOP Conf. Ser. Mater. Sci. Eng. **571** (2019) 1. https://doi.org/10.1088/1757-899X/571/1/012116
36 A. Jamal, M. M. Raahman, S. B. Khan, M. M. Abdullah, M. Faisaal, A. M. Asiri, A. Aslam, P. Khan, and K. Akhtar: J. Chem. Soc. Pak, **35** (2013) 570.